IEEE/CSC & ESAS SUPERCONDUCTIVITY NEWS FORUM (global edition), October 2016.
ASC 2016 - Student Paper Contest – 3rd Prize preprint and presentation: 1SPOr1A. Submitted to *IEEE Trans. Appl. Supercond.* for possible publication.

Screening Current-Induced Magnetic Field in a Non-Insulated GdBCO HTS coil for the 24 T All-Superconducting Magnet

Lei Wang, Qiuliang Wang, *Member, IEEE*, Jianhua Liu, Hui Wang, and Xinning Hu

***Abstract*—A 24 T all-superconducting magnet, comprising of a 9 T GdBCO high temperature superconducting (HTS) inner coil and 15 T low temperature superconducting (LTS) outer coils, has been manufactured and tested at Institute of Electrical Engineering, Chinese Academy of Sciences. The screening current generated in the GdBCO HTS coil causes a central magnetic field reduction and drift in the superconducting magnet system. Hence, it is crucial to estimate the screening current-induced magnetic field in the HTS coil. In this paper, the magnetic field generated by the screening current was numerically calculated based on magnetization analysis. To verify the simulations, related experiments were performed by three different cases at 4.2 K: i) Charging the HTS coil at different ramping rates; ii) Charging the LTS coils with central field of 10.82 T firstly and the HTS coil subsequently; iii) Charging the LTS coils with central field of 15 T firstly and the HTS coil subsequently;. The calculation results show a good agreement with the measured data.**

***Index Terms*— Non-insulated HTS insert, screening current, numerical simulation, characteristic resistance**

I. Introduction

The REBCO HTS coils have been widely used in Nuclear Magnetic Resonance (NMR) magnets beyond 1 GHz[1],[2] because of their excellent current-carrying capacities under high magnetic field. However, there will be a screening current [3]-[9] flowing in the REBCO superconducting tape, which is induced by the magnetic field perpendicular (radial direction of the coil) to the tape width while the high temperature superconducting (HTS) coil is ramped up/down or exposed to an external magnetic field. The magnetic field induced by screening current results in a central field reduction in the superconducting magnet after the coil is charged. And also, the relaxation of the field reduction with time due to the flux creep motion is harmful for the field homogeneity of the high accuracy NMR magnet. The spatial homogeneity and temporal stability, which are important for the applications of MRI and NMR, will be deteriorated by the screening current. To design a reliable superconducting magnet system, it is crucial to estimate the screening current-induced magnetic field (field reduction) in the REBCO HTS insert.

Recently, many research have been conducted on the screening current-induced magnetic field (SCIF) in the insulated or non-insulated REBCO HTS single pancake and coils [10]-[20]. However, the SCIF in non-insulated GdBCO HTS insert under a LTS outsert, especially for the superconducting magnet with high central field, is still unclear. Fully understanding the filed reduction induced by the screening current is one of the important key points to develop high accuracy NMR magnet with central field above 30 T in the future.

In this paper, numerical and experimental analyses on the central magnetic field reduction in a GdBCO HTS insert for the 24 T all-superconducting magnet were conducted. A numerical method developing from magnetization analysis in a thin film [21] is adopted to calculate the SCIF. The charging experiments of the HTS insert were carried out under a LTS outsert with central field of 0 T, 10.72 T, and 15 T, respectively. Furthermore, the effect of ramping rate on the SCIF was investigated at 4.2K (liquid helium bath). The simulation results are compared with the experimental data, which shows a good agreement.

II. Experimental Setup

A. Design of GdBCO HTS Insert and LTS Outsert

The 24 T all-superconducting magnet consists of a GdBCO HTS insert and a LTS outsert, which is comprised of 4 Nb3Sn coils and 3 NbTi coils. The LTS outsert is cooled at 4.2 K under atmospheric pressure by using liquid helium bath, and an operating current of 215.5 A could generate a central magnetic field of 15 T in a 160 mm diameter cold bore [22].

The GdBCO HTS coated conductor produced by SUNAM Inc was chosen to wind the HTS coil. The width and thickness of the GdBCO conductor are about 4.2 mm and 0.155 mm, respectively. The inner diameter, outer diameter, and height of the GdBCO HTS coil are 36 mm, 104.2 mm and 150 mm, respectively. The GdBCO HTS coil consists of 15 double pancakes and each one has 220×2 turns. There is no turn-to-turn insulations in a single pancake. The configuration of the GdBCO HTS insert is shown in Fig. 1.

This work was supported by the National Natural Science Foundation of China under Grant 50925726 and Grant 10755001 and by the National Major Scientific Equipment R&D Project under Grant ZDYZ2010-2 *(Corresponding author: Qiuliang Wang.)*

L. Wang, Q. Wang, J. Liu, H. Wang, and Xinning Hu are with the Key Laboratory of Applied Superconductivity, Institute of Electrical Engineering, Chinese Academy of Sciences, Beijing 100190, China, and also with the University of Chinese Academy of Sciences, Beijing 100083, China (e-mail: wanglei@mail.iee.ac.cn; qiuliang@mail.iee.ac.cn).

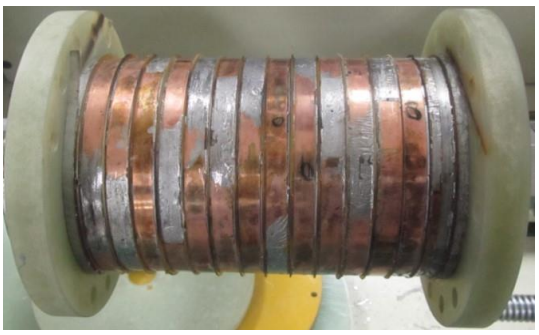

Fig. 1. Configuration of the GdBCO HTS insert

B. Equivalent Circuit Model of GdBCO HTS Insert

For the HTS coils with turn-to-turn insulations, the field reduction induced by the screening current could be determined at the time when the operating current reached at the target value. However, in the non-insulated HTS coil, there is still an I_r when the operating current reached the target value due to the typical charging/discharging delay. Prior to determining the SCIFs in the HTS insert after it is charged, the charging delay should be simulated firstly. The equivalent circuit model of the non-insulation coil is shown in Fig. 2, which is connected with a switch, a DC power supply, and a shunt resistor.

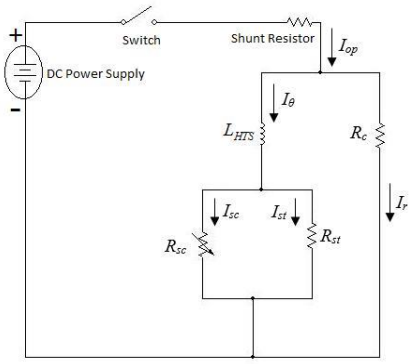

Fig. 2. Equivalent Circuit Model of the GdBCO HTS insert

The equivalent circuit model could be described by the following equations (1):

$$\begin{aligned} &L_{HTS}\frac{dI_\theta}{dt}+V_c\left(\frac{I_{sc}}{I_c}\right)^n = I_r R_c \\ &V_c\left(\frac{I_{sc}}{I_c}\right)^n = I_{st}R_{st} \\ &I_{st}+I_{sc}+I_r = I_{op} \end{aligned} \tag{1}$$

Where L_{HTS} is the self-inductance of the non-insulated HTS coil. I_θ, I_r, I_{sc}, and I_{st} are the current flowing through the spiral direction, radial direction, superconducting film, and stabilizer layer in the HTS coil, respectively. R_c and R_{st} are the characteristic resistance of the non-insulated coil and the stabilizer resistance, respectively. V_c, n, I_{op}, and I_c are the voltage criterion (10^{-4} V/m), n-value, operating current input from the power supply, and critical current of the GdBCO HTS coil, respectively. Because the experiment was conducted below the critical current and temperature, the azimuthal resistance, including matrix resistance and index loss, is assumed to be zero to facilitate the calculations [23]-[24]. Then, (1) could be simplified by (2)

$$\begin{aligned} &L_{HTS}\frac{dI_\theta}{dt} = I_r R_c \\ &I_\theta + I_r = I_{op} \end{aligned} \tag{2}$$

A sudden discharge test was carried out at 77 K (liquid nitrogen bath) to obtain R_c of the HTS insert. During the test, I_{op} increased to 20 A at a charging rate 0.1 A/s, and maintained at 20 A constantly during steady-state operation for 2000 s, then cut off. The time constant τ of the HTS insert is defined as the time at the normalized B_z of 1/e, *i.e.*, 69 s as shown in Fig. 3.

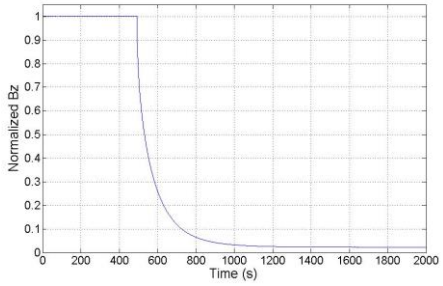

Fig. 3. Normalized B_z versus time during the discharging test

The self-inductance of the HTS insert L_{HTS} is 0.87 H. Then, the characteristic resistance could be determined by (3) as 12.61 mΩ.

$$R_c = L_{HTS} / \tau \tag{3}$$

By adding R_c into the equivalent circuit model, the time when I_r decreases to zero could be determined by (2).

III. Simulation Method

Prior to calculating the central field reduction induced by the screening current in the HTS insert, the current distribution should be determined firstly. The 30 single pancakes are labeled as i=1, 2, 3,…., 30. Each turn in the ith layer is modeled as a concentric ring and labeled as j=1,2,3,…., 220. The width of each turn $2w_0$ is discretized into N points, labeled as k=1, 2, 3,…, N. Because the aspect ratio of the GdBCO coated conductor is large, the current distribution along the thickness direction is assumed to be uniform. The simulation model for the HTS insert is shown in Fig. 4. The radial and axial directions are labeled as x-axis and y-axis, respectively.

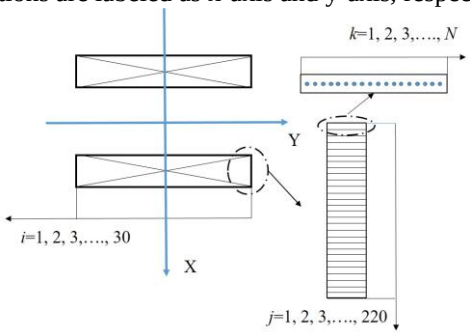

Fig. 4. Simulation Model of the GdBCO HTS insert

When the GdBCO HTS insert is charged into a transport current I_t, each turn will also be exposed to an external magnetic field generated by other turns of the HTS insert. Hence, the transport current distribution in a certain turn is

nonuniform and asymmetrical to the conductor center. The magnitude and direction of the transport current and external field will determine the current flowing directions at two sides of a certain conductor. At the *j*th turn in the *i*th layer, the criterion $m(i,j)$ for judging the effect of the external magnetic field $B_r(i,j)$ and transport current I_t is shown in (4)

$$m(i,j)=\frac{I_t}{I_c(i,j)}-\tanh\left(\frac{B_r(i,j)}{B_p(i,j)}\right) \tag{4}$$

Where $B_r(i,j)$ is the radial magnetic field, $B_p(i,j)$ and $I_c(i,j)$ are the full penetration field and critical current, respectively. $I_c(i,j)$ depends on the magnitude and direction of the external magnetic field. If $m(i,j)>0$, the current will flow in the same direction at two sides of the conductor, the azimuthal current density $J(i,j,k)$ at the *k*th point in *i*th layer and *j*th turn is determined by (5). If $m(i,j)<0$, the current will flow in different directions at two sides of the conductor, $J(i,j,k)$ should be calculated by (6) [21].

$$\begin{aligned}
&J(i,j,k)=\frac{J_c(i,j)}{\pi}[H-L+\pi] && |y(i,j,k)-p|<a\\
&J(i,j,k)=J_c(i,j) && -w_0<y(i,j,k)<p-a;\ p+a<y(i,j,k)<w_0\\
&H=\arcsin\left(\frac{(y(i,j,k)-p)\cdot(w_0-p)-a^2}{a\cdot(w_0-y(i,j,k))}\right)\\
&L=\arcsin\left(\frac{(y(i,j,k)-p)\cdot(w_0+p)+a^2}{a\cdot(w_0+y(i,j,k))}\right)
\end{aligned} \tag{5}$$

$$\begin{aligned}
&J(i,j,k)=\frac{J_c(i,j)}{\pi}[H+L] && |y(i,j,k)-p|<a\\
&J(i,j,k)=J_c(i,j) && -w_0<y(i,j,k)-p<-a\\
&J(i,j,k)=-J_c(i,j) && a<y(i,j,k)-p<w_0
\end{aligned} \tag{6}$$

Where *p* and *a* are the center position (CP) and half width (HW) of the field invariant region at the *j*th turn in the *i*th layer, respectively. *p* and *a* could be determined by (7)

$$\begin{aligned}
&p=w_0(I_t/I_c(i,j))\tanh(B_r(i,j)/B_p(i,j))\\
&a=(w_0/\cosh(B_r(i,j)/B_p(i,j)))\sqrt{1-(I_t/I_c(i,j))}
\end{aligned} \tag{7}$$

When the LTS outsert is charged first, the conductors are initial in a virgin state, firstly exposed to an radial field $B_1(i,j)$ generated by the LTS outsert, the current density $J_1(i,j,k)$ could be obtained by (8)

$$\begin{aligned}
&J_1(i,j,k)=\frac{-2J_{c(i,j)}}{\pi}\cdot\arctan\left(\frac{y(i,j,k)}{w_0}\sqrt{\frac{w_0^2-a_1^2}{a_1^2-y(i,j,k)^2}}\right) && -a_1<y(i,j,k)<a_1\\
&J_1(i,j,k)=-J_{c(i,j)} && a_1<y(i,j,k)<w_0\\
&J_1(i,j,k)=J_{c(i,j)} && -w_0<y(i,j,k)<-a_1\\
&a_1=w_0/\cosh(B_1(i,j)/B_p(i,j))
\end{aligned} \tag{8}$$

CP locates at the conductor's center and HW is a_1. Afterwards, the HTS insert is charged and a certain turn will be subjected to a transport current I_{t2} and an external field $B_2(i,j)$ generated by other turns. There will be two different cases $m_2(i,j)>0$ or $m_2(i,j)<0$ for the effects of I_{t2} and $B_2(i,j)$. In each case, the current distribution cannot be calculated by (4)-(7) because the conductor is not from a virgin state [21].

For the case $m_2(i,j)>0$, the current distribution $J_2(i,j,k)$ could be obtained by the following simulations. When the *j*th turn in the *i*th layer is subjected to I_{t2} and $B_2(i,j)$, CF and HF are set to be p_2 and a_2, respectively. The conductor is separated into three different regions: region A ($-a<y(k_1)<p_2-a_2$), region B ($p_2-a_2<y(k_2)<p_2+a_2$), region C ($p_2+a_2<y(k_3)<w_0$), each region is discretized into *M* points. Regions A and C are saturation regions, and region B is the field invariant region. For the regions A and C, the current density could be calculated by (9):

$$\begin{aligned}
&J_2(k_1)=J_c(i)-J_1(k_1) && -a<y(k_1)<p_2-a_2\\
&J_2(k_3)=J_c(i)-J_1(k_3) && p_2+a_2<y(k_3)<w_0
\end{aligned} \tag{9}$$

The current flowing in region B, from the combining contributions of regions A and C, could be calculated by (10)

$$\begin{aligned}
&J_2(k_2)=\int_A\frac{-J_2(k_1)}{\pi}\left[\arcsin\left(\frac{\alpha(\beta+\kappa)+2Ma_2}{\gamma+\kappa}\right)-\arcsin\left(\frac{\alpha(\beta-\kappa)+2Ma_2}{\gamma-\kappa}\right)\right]\\
&\quad+\int_C\frac{J_2(k_3)}{\pi}\left[\arcsin\left(\frac{\alpha(\beta_1+\kappa_1)-2Ma_2}{\gamma_1+\kappa_1}\right)-\arcsin\left(\frac{\alpha(\beta_1-\kappa_1)-2Ma_2}{\gamma_1-\kappa_1}\right)\right]\\
&\alpha=2M(y(k_2)-p_2)\\
&\beta=2M(y(k_1)-p_2) \quad \beta_1=2M(y(k_3)-p_2)\\
&\kappa=w_0+p_2-a_2 \quad \kappa_1=w_0-p_2-a_2\\
&\gamma=2M(y(k_1)+y(k_2)) \quad \gamma_1=2M(y(k_3)-y(k_2))
\end{aligned} \tag{10}$$

I_t is equal to the summation of discretized current densities over the conductor's cross-section and $B_2(i,j)$ is equal to the radial magnetic field generated at point p_2 by the other points in the conductor. Then, the current and field equations could be obtained by (11)

$$\begin{aligned}
&I_t=\frac{2w_0d_0}{N}\int_{-w_0}^{w_0}J_2(k)\\
&B_2(i,j)=\frac{\mu_0d_0}{2\pi}\int_{-w_0}^{w_0}\frac{J_2(k)}{y(k)-p_2}
\end{aligned}. \tag{11}$$

The two unknowns p_2 and a_2 could be obtained by solving (11). Adding p_2 and a_2 into (8)-(10), the $J_2(i,j,k)$ is obtained. So, the final current density $J_3(i,j,k)$ is equal to the sum of $J_2(i,j,k)$ and $J_1(i,j,k)$.

The central axial magnetic field of the GdBCO HTS insert is the sum of contributions from all of the points, and can be calculated by (12)

$$B_c=\sum B_c(i,j,k)=\frac{\mu_0J(i,j,k)w_0d_0x(i,j,k)^2}{N(x(i,j,k)^2+y(i,j,k)^2)^{3/2}} \tag{12}$$

Where μ_0 is the magnetic permeability. The HTS insert constant (axial filed per ampere at center) B_0 is 0.0536 T/A. Then the simulated central magnetic field reduction B_{fr} in the GdBCO HTS insert could be calculated by $B_{fr}=B_0*I_t-B_c$.

IV. Results And Discussions

In order to study the central magnetic field reduction in the GdBCO HTS insert, three different charging tests were performed in a bath of liquid Helium.

A. Charging the HTS insert only

In this case, the HTS coil was charged following two series. The 1st series is charged from 0-160 A by the following sequences: 0 A -10 A, 10 A -20 A, 20 A -30 A, 30 A - 40 A,

40 A -60 A, 60 A -80 A, 80 A - 100 A, 100 A - 110 A, 110 A - 120 A, and 120 A - 140 A at a rate of 0.1 A/s, 140 A - 160 A at a rate of 0.05 A/s. The 2nd series is charged from 0-200 A by the following sequences: 0-120 A (0.05 A/s), 120 A -140 A (0.03 A/s), 140 A -160 A and 160 A -161.7 A (0.015 A/s), 161.7 A -180 A, 180 A - 190 A, and 190 A - 200 A (0.01 A/s). For all of the cases, the operating current was held for 700 s between each two sequences, which is the time when the simulated I_r decreases to zero through (2). Then the center magnetic field B_m is measured by a Hall sensor.

The tested B_{fr} induced by the screening current for the 1st and 2nd series is shown by the circles and asterisks in Fig. 5, respectively. The central filed reductions of the 1st and 2nd charging series at I_{op}=120 A, 140 A, 160A are 0.57 T, 0.67 T, 0.6885 T and 0.581 T, 0.653 T, 0.6766 T, respectively. The charging rates of the 1st and 2nd charging series at I_{op}=120 A, 140 A, 160A are 0.1 A/s, 0.1 A/s, 0.05 A/s and 0.05 A/s, 0.03 A/s, 0.015 A/s, respectively. B_{fr} is not affected by the ramping rate of the HTS insert. When the operating current is larger than 170 A, B_{fr} tends to be saturated. The largest B_{fr} is 0.7034 T and the ratio of B_{fr}/B_c is 6.2%.

B. Charging the LTS coil with a center field of 10.72 T firstly and the HTS coil subsequently

In this section, the LTS outer was charged from 0 A -154 A firstly, corresponding to a central field of 10.82 T. Afterwards, the HTS insert was charged from 0 A to 160 A by the following sequences: 0 A - 60 A, 60 A - 100 A at a ramping rate of 0.05 A/s, 100 A - 150 A at a rate of 0.03 A/s, 150 A - 160 A at 0.01 A/s. The results are shown by the squares in Fig. 5. B_{fr} at I_{op}= 60 A, 100 A, 150 A, and 160 A are 0.2364 T, 0.4079 T, 0.4731 T, and 0.4785 T, respectively. The ratios of B_{fr}/B_c are 7.16%, 7.42%, 5.73%, and 5.44%, respectively. The experimental data shows that, although B_{fr} increases with the operation current, the ratio of B_{fr}/B_c decreases with I_{op} when the operating current is larger 100 A.

C. Charging the LTS coil with a center field of 15 T firstly and the HTS coil subsequently

In this section, the LTS outer was charged from 0 A - 215.5 A firstly, corresponding to a central field of 15 T. Then, the HTS insert was charged from 0 A to 150 A by the following sequences: 0 A - 60 A, 60 A - 100 A at a ramping rate of 0.03 A/s, 100 A - 150 A at 0.02A/s. The results are shown by the triangles in Fig. 5. B_{fr} at I_{op}= 60 A, 100 A, and 150 A are 0.0565 T, 0.1488 T, and 0.1673 T, respectively. The ratios of B_{fr}/B_c are 1.71%, 2.7%, and 2.03%. B_{fr} tends to be saturated after the operation current is larger than 100 A.

D. Discussions

The simulation results are compared with the experimental data of the three cases mentioned above as shown in Fig. 5. While I_{op}=60 A, 100 A, and 150 A, B_{fr} and B_{fr}/B_c are summarized in Table I for the LTS outsert with central field of 0 T, 10.82 T, and 15 T, respectively. B_{fr} decreases with the central field of LTS outsert increasing, the reductions of B_{fr} will increase with the operation current while the reductions of B_{fr}/B_c decreases with I_{op} increasing. When the operation current is 150 A, B_{fr} in the LTS outsert with central field of 15 T is 75% less than that of B_{fr} in the LTS outsert with central field of 0 T, the suppression for B_{fr} is significant while the central field of LTS outsert increases from 0 T to 15 T.

TABLE I THE RESULTS OF B_{FR} AND B_{FR}/B_C

No.	60 A	100 A	150 A
LTS (0 T)	0.3025 T (9.1667%)	0.4915 T (8.9364%)	0.667 T (8.0848%)
LTS (10.82T)	0.2364 T (7.1636%)	0.4079 T (7.4164%)	0.4731 T (5.7345%)
LTS (15 T)	0.0565 T (1.7121%)	0.1488 T (2.7055%)	0.1673 T (2.0279%)

The simulation results agree well with the experimental data except that I_{op} is larger than 180 A when the central field of LTS outsert is 0 T. Because the critical current density distribution is assumed to be uniform along the conductor's width in the numerical calculation, but it distributes nonuniformly along the real conductor's width if the conductor is discretized into N points. In some points, the critical current density is larger than the average one, which causes the calculated B_{fr} less than the tested one. The decreasing of simulated value is more significant for cases that the central field of LTS outsert increases. The simulation model will be improved in the future to increase the accuracy.

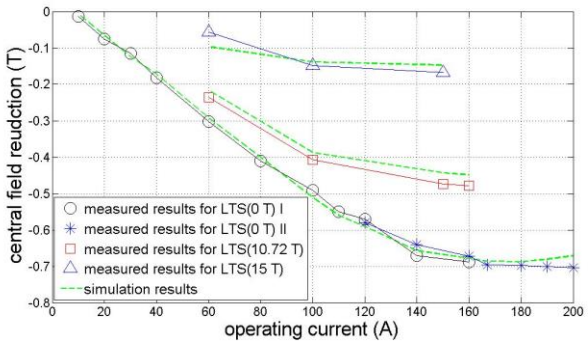

Fig. 5. Comparison of measured and simulation results

V. CONCLUSIONS

The screening current induced magnetic field in a non-insulated GdBCO HTS insert for the 24 T all-superconducting magnet is studied through the numerical simulations and charging test. Based on the experimental and numerical results, the conclusions are summarized as follows: 1) The simulation results show a good agreement with the experimental data except that the operating current is more than 180 A. 2) When the central field of LTS outsert increases, the central filed reduction decreases sharply as large as 75 % (from 0.667 T to 0.1673 T) while the operating current is 150 A. The suppression is significant. 3) The central filed reduction is not affected by the ramping rate of the operation current. The results will provide an important reference to quantify the SCIF in the non-insulated GdBCO HTS insert, which could help us design and fabricate a 15 T non-insulated HTS insert for the 30 T all-superconducting magnet in the future.

REFERENCES

[1] Y. Koyama, T. Takao, Y. Yanagisawa, H. Nakagome, M. Hamada, T. Kiyoshi, M. Takahashi, T. Yamazaki, and H. Maeda, "Towards beyond 1 GHz NMR: Mechanism of the long-term drift of screening current-induced magnetic field in a Bi-2223 coil," *Physica C.* vol. 469, no. 13, pp. 694–701, Jul. 2009.

[2] N. Amemiya and K. Akachi, "Magnetic field generated by shielding current in high Tc superconducting coils for NMR magnets," *Supercond. Sci. Technol.*, vol. 21, no. 9, Jun. 2008, Art. No. 095001.

[3] G. Chen, T. Qu, and Z. Han, "Measurement and calculation of residual Magnetic field in a Bi2223/Ag Magnet," *IEEE Trans. Appl. Supercond.*, vol. 17, no.2, pp. 2394-2397, Jun. 2007

[4] E. H. Brandt, "Thin superconductors in a perpendicular magnetic ac field: General formulation and strip geometry," *Phys. Rev. B*, vol. 49, no. 13, pp. 9024-9040, Apr. 1994.

[5] E. H. Brandt, "Superconductors of finite thickness in a perpendicular magnetic field: Strips and slabs," *Phys. Rev. B*, vol. 54, no. 6, pp. 4246-4264, Mar. 1996.

[6] T. Yazawa, J. J. Rabbers, B. T. Haken, H. H. J. Kate, and Y. Yamada, "Numerical calculation of current density distributions in high temperature superconducting tapes with finite thickness in self field and external field," *Physica C*, vol.310, no. 1-4, pp. 36-41, Dec. 1998.

[7] H. Maeda and Y Yanagisawa, "Recent developments in high-temperature superconducting magnet technology (Review)," *IEEE Trans. Appl. Supercond.*, vol. 24, no. 3, pp. 1-12, Jun. 2014.

[8] K. Kajikawa, and K. Funaki, "A simple method to eliminate shielding currents for magnetization perpendicular to superconducting tapes wound into coils," *Supercond. Sci. Technol.*, vol. 24, no. 12, Dec. 2011, Art. No. 125005

[9] Y. Yanagisawa, H. Nakagome, Y. Koyama, R. Hu, T. Takao, M. Hamada, T. Kiyoshi, M. Takahashi and H. Maeda, "Effect of current sweep reversal on the magnetic field stability for a Bi-2223 superconducting solenoid," *Physica C*, vol.469, no. 22, pp. 1996-1999, Nov. 2009.

[10] D. G. Yang, K. L. Kim, Y. H. Choi, O. J. Kwon, Y. J. Park, and H. J. Lee, "Screening current-induced field in non-insulated GdBCO pancake coil," *Supercond. Sci. Technol.*, vol. 26, no. 10, Oct. 2013, Art. No. 105025.

[11] M. Ahn, T. Yagai, S. Hahn, R. Ando, H. Bascunan, and Y. Iwasa, "Spatial and Temporal Variations of a Screening Current Induced Magnetic Field in a Double Pancake HTS insert of an LTS/HTS NMR Magnet," *IEEE Trans. Appl. Supercond.*, vol. 19, no.3, pp. 2269–2272, Jun. 2009

[12] A. Matsumi et al, "Evaluation of Irregular Magnetic Field Generated by Screening Current in REBCO coils for High Accuracy Field," *IEEE Trans. Appl. Supercond.*, vol. 26, no.4, Jun. 2016, Art. No. 4702305

[13] A. Mochida et al, "Evaluation of Magnetic Field Distribution by Screening current in Multiple REBCO coils," *IEEE Trans. Appl. Supercond.*, vol. 26, no.4, Jun. 2016, Art. No. 4702805

[14] S. Hahn, J. Bascunan, W. Kim, E. Bobrov, H. Lee, and Y. Iwasa, "Field Mapping, NMR Lineshape, and Screening currents Induced Field Analyses For Homogeneity Improvement in LTS/HTS NMR Magnets," *IEEE Trans. Appl. Supercond.*, vol. 18, no.2, pp. 856–859, Jun. 2008

[15] R. Itoh, Y. Oga, S. Noguchi, and H. Igarashi, "Screening Current Simulation Inside YBCO tape in Charging YBCO Magnet", *IEEE Trans. Appl. Supercond.*, vol. 23, no.3, Jun. 2013, Art. No. 4600905

[16] Q. L. Wang, *Practical Design of Magnetostatic Structure Using Numerical Simulation*, Hoboken, NJ, USA: Wiley, 2013.

[17] Y. Kim, Y. Hyuck, D. Yang, H. Shin, M. Cheol, and H. Lee, "Study for Reducing the screening current Induced Field in a 10-MHZ NO-Insulation Magnet Using Current Sweep Reversal Method" *IEEE Trans. Appl. Supercond.*, vol. 25, no.3, Jun. 2015, Art. No. 4601005

[18] S. Hahn, J. Bascunan, W. Kim, E.S. Bobrov, H. Lee and Y. Iwasa, "Field Mapping, NMR Lineshape, and Screening currents induced field analyses for homogeneity improveen in LTS/HTS NMR magnets," *IEEE Trans. Appl. Supercond.*, vol. 18, no.2, pp. 856-59, Jun. 2008

[19] A. Otsuka, Y. Yanagisawa, T. Kiyoshi, H. Maeda, H. Nakgome, and T. Takeda, "Evaluation of the screening current in a 1.3 GHz NMR Magnet Using ReBCO," *IEEE Trans. Appl. Supercond.*, vol. 21, no.3, pp. 2076–2079, Jun. 2011

[20] S. Iwai et al, "Experimental Results of Screening current Field with 10 T Class Small REBCO coil," *IEEE Trans. Appl. Supercond.*, vol. 26, no.4, Jun. 2016, Art. No. 4302305

[21] E. Zeldov, J. R. Clem, M. McElfresh, and M. Darwin, "Magnetization and transport currents in thin superconducting films," *Physical Review B*, vol. 49, no. 14, pp. 9802-9822, Apr. 1994.

[22] Q. Wang, J. Liu, S. Song, G. Zhu, Y. Li, X. Hu, and L. Yan, " High Temperature Superconducting YBCO Insert for 25 T Full Superconducting Magnet", *IEEE Trans. Appl. Supercond.*, vol. 25, no. 3, Jun. 2015, Art. No. 4603505.

[23] S. Hahn, D. Park, J. Bascunan, and Y. Iwasa, "HTS pancake Coils without turn-to-turn Insulation", *IEEE Trans. Appl. Supercond.*, vol. 21, no.3, pp. 1592–1595, Jun. 2011

[24] K. Kim et al, "Effect of Winding Tension On Eleetrical Behavior Of a No-Insulation ReBCO Pancake Coil", *IEEE Trans. Appl. Supercond.*, vol. 24, no.3, Jun. 2014, Art. No. 4600605